Experiments in Fluids 7, 157–163 (1989)

Experiments in Fluids

Optical tomography applied to speckle photographic measurement of asymmetric flows with variable density*

T. C. Liu**, **W. Merzkirch** and **K. Oberste-Lehn**

Lehrstuhl für Strömungslehre, Universität Essen, D-4300 Essen, F. R. Germany

Abstract. Optical tomography is applied to the speckle photographic measurement of an asymmetric flow field with variable fluid density. The convolution back projection algorithm is used for obtaining the 3-D density distribution. Noise in the experimental data is reduced by spline smoothing. The method is verified with a steady, laminar, axisymmetric helium jet exhausting vertically into the ambient air, and then applied to a non-axisymmetric helium jet for determining the helium concentration. It is found that speckle photographic recordings are very adequate for tomographic reconstruction, because they provide a high number of data points from each projection. The influence of the limited number of projections on the reconstruction quality is particularly investigated.

1 Introduction

The refractive deflection of rays in a light beam, which is transmitted through a flow with variable refractive index or fluid density, can be measured by means of speckle photography, as it has been shown by Köpf (1972) and Debrus et al. (1972). The method has been developed by Wernekinck and Merzkirch (1987) for application to spatially extended flow fields. For, virtually, any point of the field of view, (x, y), the deflection angle can be determined from a measurement of the displacement of the respective light ray in the recording plane. Since the displacement is measured as a vector, the two components of the deflection angle, ε_x and ε_z, are determined simultaneously. Under the assumption that the light beam propagates through a gas flow in the y-direction, the deflection angle is related to the gas density ϱ by (e.g., Merzkirch 1987)

$$\varepsilon_x = K \int \frac{\partial \varrho}{\partial x}\, dy, \qquad \varepsilon_z = K \int \frac{\partial \varrho}{\partial z}\, dy, \tag{1}$$

where K is the Gladstone-Dale constant of the gas, and the integral is taken along the path of a ray in the test field. In general, ϱ is a function of the three space coordinates x, y, z, and the information on the dependence of ϱ on y is lost, as in any line-of-sight method, due to the above integration.

Computerized tomography is a possible means for extending the capability of optical line-of-sight methods to the measurement of three-dimensional flow fields (e.g., Hesselink 1989). This technique requires that recordings with the respective optical method be taken in different viewing directions ("projections") covering 180° at equal intervals (or less than 180° if the flow exhibits a certain kind of symmetry or if other information on the test field is known). Several algorithms are available for reconstructing the three-dimensional density field from the information recorded in the various projections. Successful reconstructions of the density distribution in 3-D gas flows have been performed by combining tomography with holographic interferometry (e.g., Sweeney and Vest 1973; Snyder and Hesselink 1984) or optical beam deflectometry (Faris and Byer 1987).

For a given test object, the quality of the tomographic reconstruction depends on the number of projections taken, the covered total angular range of viewing directions, and the amount of information (density of data or number of data points per square unit) available from each projection. The speckle photographic method is particularly attractive, because it can provide a relatively high data density from each projection, higher than any interferometric method. The aim of the present investigations was to adopt the tomographic technique to the speckle photographic measurement of light deflection in a 3-D flow with variable density. The test object to which the method is applied is a steady laminar jet of helium exhausting in vertical direction into the ambient air. Reconstructions based on the method of convolutions (Herman 1980) are determined from 4 to 12 separate projections. For the purpose of comparing the technique with reference data, the method was first applied to an axisymmetric jet. A similar situation has been studied by Blinkov et al. (1987). Then, experiments were performed with a non-axisym-

* Dedicated to Professor Dr.-Ing. J. Zierep on the occasion of his 60th birthday

** Present address: Guangzhou Institute of Energy Conversion, Academia Sinica, Guangzhou, P. R. China

metric flow field, and the influence of the number of projections on the quality of the reconstruction was particularly investigated.

2 Algorithm of tomographic reconstruction from speckle photographic recordings

The 3-D density field of the helium jet under study can be considered as being composed of a set of 2-D density distributions at cross sections perpendicular to the axis of the jet. Once the density distributions at different cross sections can be reconstructed from the data available in the specklegrams, the 3-D density field can be established by simply piling up the 2-D density distributions for the different cross sections. The problem of reconstructing the 3-D density field therefore reduces to the reconstruction of a set of 2-D density fields from 1-D line-integrated data on light deflection angles obtained in the specklegrams.

The geometry, adopted in our analysis, is shown in Fig. 1 for a cross section normal to the vertical z-axis, which is the direction of the jet flow. The x and y coordinates refer to the flow field, while the light transmitted through the jet passes along the t-direction, normal to the z-axis. The photographic plate on which the speckle patterns are recorded is a plane normal to the t-axis, i.e., parallel to the s-axis. Specklegrams at different viewing directions can be taken by rotating the jet (x-y coordinates) or the optical set-up (s-t coordinates), or with a multidirectional optical arrangement.

The helium jet exhausts from a nozzle into the ambient air, which is entrained into the jet and mixes with the helium. The aim of the experiments is to measure the concentration of helium in the mixing region. Let a quantity ϱ^* be defined as

$$\varrho^* = (n_{a0} - n)/(n_{a0} - n_{h0}), \tag{2}$$

where n_{a0}, n_{h0} and n are, respectively, the refractive indices of ambient air, pure helium and the mixture of air and helium in the jet at atmospheric pressure and room temperature. By using the Gladstone-Dale formula and the ideal gas law,

$$n_{a0}(1 - \varrho^*) + n_{h0}\varrho^* = K_a \varrho_a + K_h \varrho_h + 1 \tag{3}$$

$$R_a \varrho_a + R_h \varrho_h = R_h \varrho_{h0}, \tag{4}$$

it can be shown that ϱ^* is just the relative helium density in the mixture:

$$\varrho^* = \varrho_h/\varrho_{h0}. \tag{5}$$

ϱ_a, ϱ_h, ϱ_{h0} are, respectively, the partial densities of air and helium in the mixture, and the density of pure helium at atmospheric pressure and room temperature, and K_a, K_h, R_a, R_h are, respectively, the Gladstone-Dale constants and the gas constants of air and helium. The limiting values of ϱ^* are $\varrho^* = 1$ for pure helium and $\varrho^* = 0$ for pure air.

A light ray propagating along a line $s = \text{const.}$ with

$$s = s_m = x \cos\theta_1 + y \sin\theta_1 \tag{6}$$

is locally deflected by an angle ε given by

$$d\varepsilon/dt = \partial (n/n_{a0} - 1)/\partial s. \tag{7}$$

Here, the light ray is assumed to propagate along a straight trajectory, and the fact has been recognized that the change in refractive index in the mixture is small compared to the indices of air or helium. Equation (7) can be rewritten in terms of the relative helium density ϱ^* as

$$\varepsilon(s, \theta) = \int \partial\varrho^*/\partial s \, dt, \tag{8}$$

where the integral is taken along the line $s = s_m$. This is the basic equation for the reconstruction of the relative helium density ϱ^* from experimental data ε obtained in each projection.

There are many reconstruction algorithms available for optical tomography. The most familiar algorithms are the algebraic reconstruction technique (ART) and the convolution backprojection method (e.g., Herman 1980; Hesselink 1989). The latter algorithm has been proved to consume less computing time and to be less sensitive to the noise in the experimental data. For these reasons the convolution backprojection algorithm has been chosen in our case for the reconstruction of the helium density field.

By taking Fourier transforms on both sides of Eq. (8) and after some rearrangements, the inverse transform gives the helium density distribution in the following form:

$$\varrho^*(x, y) = \int_0^{\pi} \varepsilon(s, \theta) * q(s) \, d\theta, \tag{9}$$

where the integrand is a convolution of the projections $\varepsilon(s, \theta)$ and a filter function $q(s)$.

Equation (9) reveals that the reconstructed density distribution is actually the filtered projections followed by backprojections from all directions of viewing angles. The filtering of the projections (convolution) accounts for a stability against noise in the experimental data. Additional filters can be designed and convolved with $q(s)$ to further reduce the noise. However, this will result in a reduction of spatial resolution in the reconstructed image.

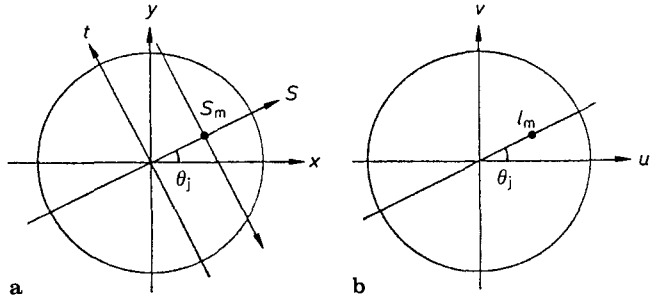

Fig. 1 a and b. Geometry of speckle photographic tomography, **a** spatial domain, **b** Fourier transform domain

In our experiments specklegrams are taken in N different viewing directions with equal angular intervals, $\Delta\theta$, and the specklegrams are evaluated along the s-direction at M points of equal spacing Δs. The equation for the reconstruction of the density $\varrho^*(x, y)$ now is required to be in a discretized form. This can be accomplished by using the trapezoidal rule. The result is

$$\varrho^*(k\Delta x, n\Delta y) = (N\pi)^{-1} \sum_{j=0}^{N-1} \sum_{m'=-(M-1)/2}^{(M-1)/2} \varepsilon(m'\Delta s, j\Delta\theta)\, q(m-m'), \quad (10)$$

where k, n, j, m and m' are integers, Δx and Δy are the grid sizes in x and y directions of the discretized reconstruction plane. The discretized filter function now is expressed as

$$q(m) = \begin{cases} 1/m, & \text{when } m \text{ is odd} \\ 0, & \text{otherwise,} \end{cases} \quad (11)$$

where $m = 0, \pm 1, \pm 2, \ldots, \pm (M-1)/2$. Details are given in the Appendix.

Because of the discretization of the reconstructed field and the limited number of projections used, interpolations between filtered projections have to be performed in order to obtain the backprojections at the desired points of the reconstructed field. A number of interpolation techniques are available for this purpose, among which a linear interpolation method was chosen for our case, because of its simplicity and low sensitivity to noise. It served to implement the interpolations between adjacent filtered projections before the backprojections were executed.

According to the projection-slice theorem, the Fourier transform of a projection along $s = s_m$ in the spatial domain (x-y) produces a point at l_m in the Fourier transform domain (u-v) (Fig. 1). Fourier transforms of an infinite number of projections taken continuously in radial and angular directions (s and θ) fill the whole Fourier transform domain. In this case the inverse Fourier transforms theoretically recover the original function in the space domain. This means that accurate reconstructions can be obtained theoretically by using an infinite number of projections. In practice, however, only a limited number of projections can be recorded in an experiment. With the automated image processing technique used in speckle photography, it is possible to increase the spatial resolution due to the possible enhancement of the sampling rate in s-direction (Fig. 1).

According to the sampling theory of signal processing, there exists a critical sampling rate, which is equal to twice the highest spatial frequency in the Fourier transform domain of the sampled object. Undersampling, at which the sampling interval is larger than the critical value, inevitably results in aliasing effects in the reconstructed image. Aliasing is one of the artifacts which may occur in the reconstructed image, and it is of great impact on the reconstruction accuracy. It describes the phenomenon that the high spatial frequency part of the object, which is cut off by undersampling, appears and superimposes to the lower frequency part of the object in the Fourier transform domain, and therefore distorts the reconstruction image. Since the object function is bounded in space and is zero outside a certain region, the spatial frequency distribution is not band-limited. This implies that the sampling intervals in radial and angular direction being not small enough will result in undersampling.

Another source of artifacts comes from the interpolation error at undersampling rate. The noise in the experimental data also contributes to part of the errors in the reconstruction image.

Numerical simulation is one of the procedures necessary for verifying the tomographic reconstruction program. It may be used for determining the proper number of projections in radial and angular directions under the aspect of reducing reconstruction artifacts, and examining the effect of noise in the projection data on the reconstruction quality. We have used a Gaussian function with elliptical cross section and two Gaussian functions located eccentrically in the reconstruction plane for simulating a helium jet with asymmetry and two jets with eccentrical locations, respectively. The line-integrated deflection angles (projections) were computed numerically by taking derivatives of the functions, and performing the numerical integrations using a fifteen-points Gaussian quadrature. Different sampling rates were considered. Noise was added to the projection data deliberately for studying the effect of the noise on the quality of the reconstruction. The simulation results confirmed that the used convolution backprojection algorithm is suitable for speckle photographic tomography, and stable with respect to the noise in the projection data. It was found in the simulation studies, that more than 8 specklegrams (angular samplings) are required for reconstructing the jet with asymmetric shape or eccentric location without significant artifacts.

3 Experiments and results

The object to be measured in the experiments was the three-dimensional density field of a steady laminar jet of helium, exhausting from a nozzle of elliptic cross-section into the ambient air at atmospheric pressure and room temperature. The nozzle was mounted vertically 3 mm off the axis of a plate which could be rotated to any desired angle with respect to the incident light direction. The size of the cross-section of the jet is 4,5 mm wide in x and 7 mm wide in y. The flow field of the jet with this geometric arrangement is obviously non-axisymmetric. The velocity of the helium jet at the nozzle exit was kept at 0.75 m/s, corresponding to a Reynolds number of 43, which provided a laminar jet. For the investigation of the effects of the asymmetry of the jet on the artifacts in the

tomographic reconstruction image, an axisymmetric helium jet, expanding from a nozzle of 6 mm in diameter and centered to the axis of the turning plate, was also measured under the same experimental conditions as those for the non-axisymmetric case.

Figure 2 shows the optical arrangement used in our speckle photographic experiment. A 35 mW He-Ne laser serves as the light source. The optical arrangement used is similar to that adopted by Wernekinck and Merzkirch (1987) for spatially extended test objects. A camera with a shutter speed of 1/4000 s was used for recording the speckle displacements, Δ, during two exposures with and without jet flow. A beam splitter provided an additional light for taking a shadowgraph of the flow pattern of the helium jet. This served for a control on whether the jet flow was stable and laminar. The turning plate was driven by a stepping motor for the desired directions of projection.

The helium jet was imaged by a lens onto a ground glass plate, from which speckles were produced by the rays from two exposures. The camera used was focused on a plane a distance l away from the ground glass and it recorded the double images of speckles, resulting from two exposures. The speckle displacements were generated by the light deflected in the jet during the exposure with flow. The choice of the distance l depends on the expected range of the spacing of the Young's fringes in the image processing of the speckle displacements (Wernekinck and Merzkirch 1987).

The relation between the speckle displacement Δ and the integrated deflection angle ε along the optical pathlength in the jet is $\varepsilon = \Delta/l$. Since the helium density derivatives with respect to the s-axis change signs along the s-direction, a reference displacement of speckles, Δ_0, was superimposed by shifting the recording camera in s-direction. This shift was added to the original displacements to distinguish the signs. The automated image processing system supported by a PDP 11/23+ minicomputer was utilized to evaluate the spatial frequencies of the Young's fringes produced by speckle displacements $\Delta + \Delta_0$ (Erbeck and Keller 1987). The data of deflection angles can be obtained by using the following simple relationship:

$$\varepsilon = C(f - f_0), \tag{12}$$

with f and f_0 being the spatial frequencies of the Young's fringes due to the helium jet and reference shift of the recording film, respectively, and C being a constant under fixed conditions in the experiment and equal to $(\lambda/B)(L/l)$. λ is the wavelength of the He-Ne laser, and B is the magnification of the optical system for recording. L is a distance between the specklegram and the screen for the video camera to pick up signals in the evaluation of the Young's fringe pattern (Fig. 3).

The helium density distribution of the non-axisymmetric jet at a cross section 5 mm above the nozzle exit plane was measured by speckle photography and reconstructed tomographically. The size of the reconstruction region was chosen to be 20 mm × 20 mm in the x, y-coordinate system. Specklegrams of up to 12 viewing angles and 199 points of evaluation along a line on each specklegram were taken to provide input data for the tomographic reconstruction program. A least-squares cubic spline approximation for data smoothing and interpolation for the in-between points were performed to obtain data of 221 points in 20 mm with noise reduction. The total amount of data from 12 specklegrams is 2652 data points for one cross section of the jet.

The tomographic reconstructions of the helium jets are shown in Figs. 4 and 5. The helium density distribution of an axisymmetric jet has been reconstructed with angular sampling numbers (projections) of 4, 6, 8 and 12 over 180°, repectively, shown by the tomograms in Fig. 4. It is obvious that the reconstructions from 8 and 12 specklegrams are of higher quality, while those with less than 8 projections include artifacts in the outer region of the reconstruction plane near the edge of the image, but still

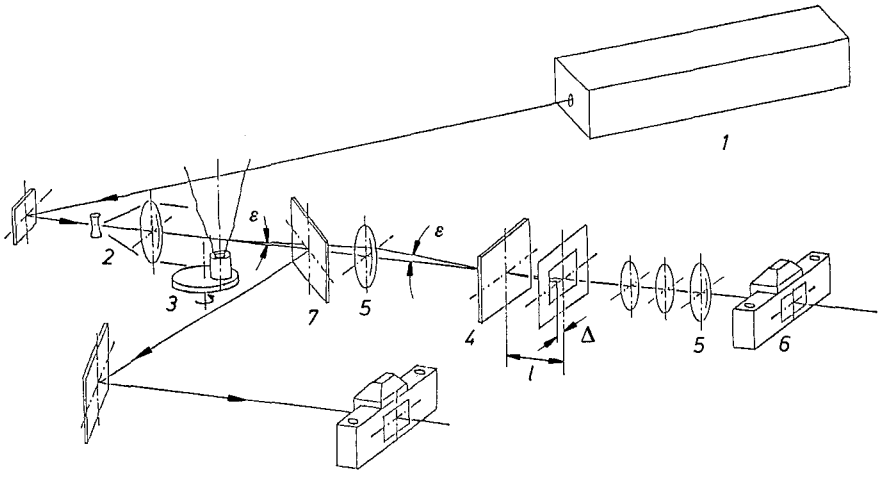

Fig. 2. Optical arrangement for tomographic speckle-photography; *1* He-Ne laser of 35 mW, *2* beam expander, *3* nozzle mounted on a turning plate, *4* ground glass, *5* imaging lenses, *6* recording camera, *7* beam splitter

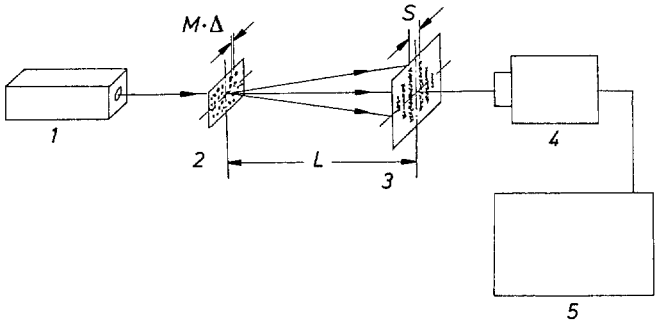

Fig. 3. Arrangement for the evaluation of Young's fringes; *1* illuminating laser, *2* specklegram, *3* screen, *4* video camera, *5* automated image processor, supported by PDP11/23+

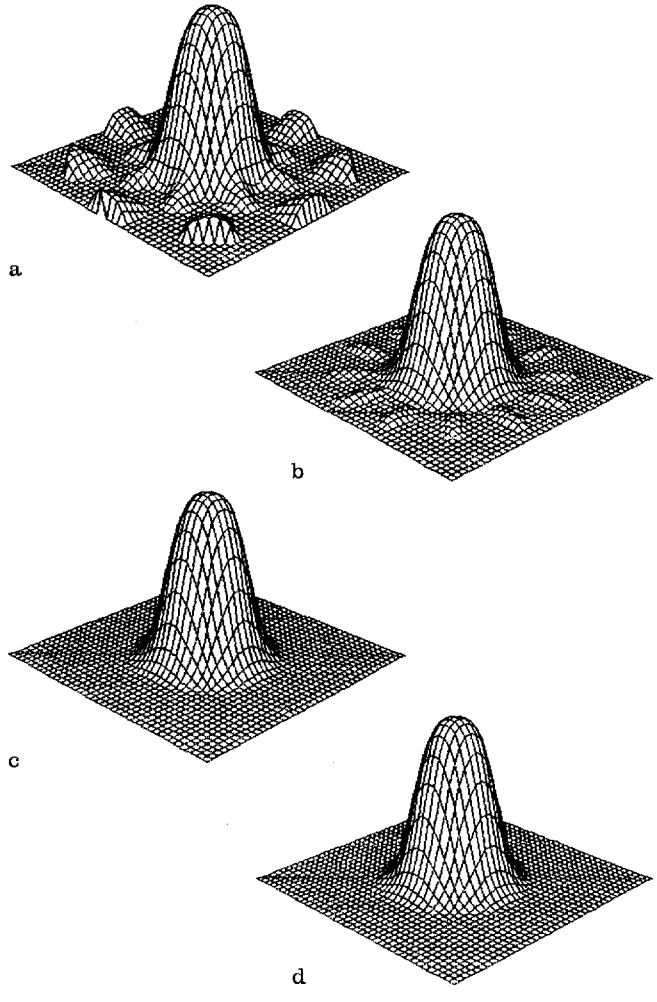

Fig. 4a–d. Tomograms of the helium density distribution of an axisymmetric jet; reconstructed with **a** 4, **b** 6, **c** 8, and **d** 12 specklegrams

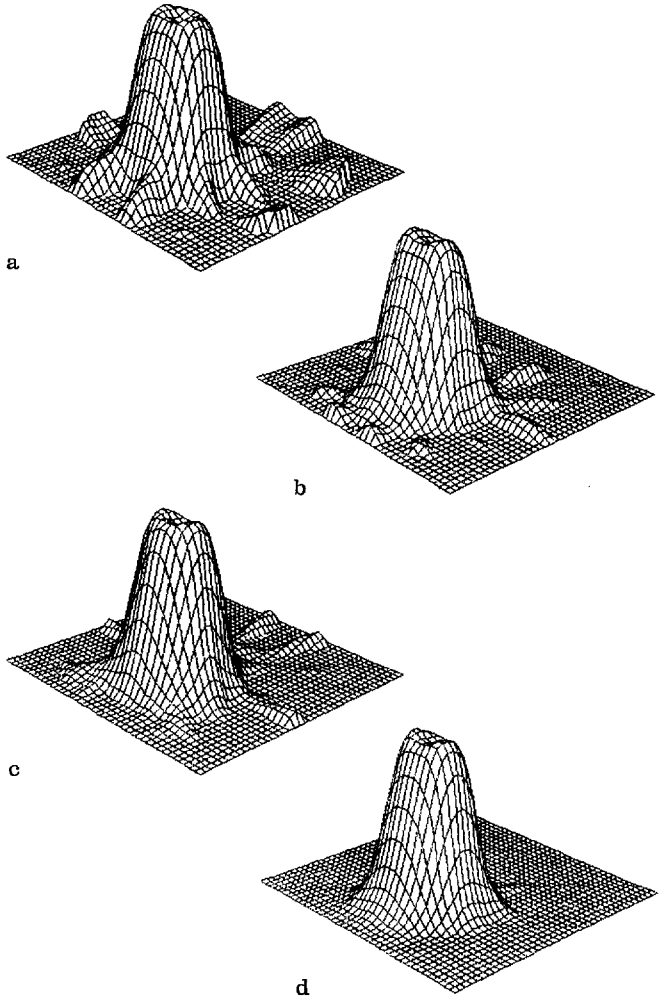

Fig. 5a–d. Tomograms of the helium density distribution in a jet of elliptic cross-section; reconstructed with **a** 4, **b** 6, **c** 8, and **d** 12 specklegrams

being of acceptable quality in the central part of the image. Tomograms of the helium density of the non-axisymmetric jet are shown in Fig. 5 again for 4, 6, 8 and 12 angular projections. From Fig. 5 it follows that only the reconstruction using 12 specklegrams is of satisfactory quality without significant aliasing effects. The reconstructions with less than 12 angular samplings show artifacts of a larger amplitude than those in the axisymmetric case (Fig. 4) and with the lack of symmetry. Figure 5 verifies that asymmetry of the flow field results in a higher number of angular samplings required for satisfactory reconstruction. We have also used the same nozzle with the elliptic cross-section, but located vertically at the center of the turning plate for experiments in order to investigate the effect of asymmetry on the reconstruction. The tomograms obtained in this case appear with more or less the same features as in the case of the jet located off-axis. It appears that for our object investigated the asymmetry

introduced by an off-axis location has no significant effect on the quality of the reconstruction. The asymmetry of the object itself is mainly responsible for the enhancement of artifacts.

The artifacts appearing in the tomograms of Figs. 4 and 5 exhibit spatial oscillations in radial and angular direction. The angular oscillations in the outer region of the reconstruction plane are the results of angular undersampling. Their peaks and valleys form streaks, the number of which is the same as the number of sampling angles. With increasing the number of angular samplings, these oscillations move away from the center and their amplitudes decrease. The radial oscillations are due to the convolving function and the interpolation. As the number of angular samplings increases to 8 for the axisymmetric case and 12 for the asymmetric case, the oscillations become too weak to be noticed. The same oscillation phenomena have been observed and demonstrated by Rowland (Herman 1980) in analyzing a point response reconstruction.

4 Conclusions

A method of tomographic reconstruction from speckle photographic recordings has been developed for measuring the three-dimensional density distribution in a laminar helium jet. The convolution backprojection algorithm has been successfully applied in the reconstruction process. Numerical simulations and reconstructions from specklegrams for both axisymmetric and non-axisymmetric cases have shown that the number of specklegrams taken in different directions at equal intervals affects the quality of the reconstruction. Artifacts originating from aliasing and interpolation errors become significant when the number of specklegrams used is less than 8 for the axisymmetric case and 12 for the asymmetric case. The noise in the experimental data has been smoothed by a cubic spline technique. This procedure improves the reconstruction quality. The results obtained demonstrate that the optical tomography extends the applicability of speckle photography to the measurement of three dimensional density fields.

Acknowledgements

Financial support of this work by Stiftung Volkswagenwerk is gratefully acknowledged. The authors thank J. Keller for his assistance in the data processing.

Appendix: Formulation of the convolution backprojection algorithm for speckle-photographic tomography

The Fourier transforms of ε and ϱ^* in Eqs. (2) and (8) are:

$$E(l,\theta) = \int_{-\infty}^{+\infty} \varepsilon(s,\theta)\, e^{-\mathrm{i}\,2\pi ls}\, ds \tag{A1}$$

$$R(l,\theta) = \iint_{-\infty}^{+\infty} \varrho^*(x,y)\, e^{-\mathrm{i}\,2\pi ls}\, ds\, dt \tag{A2}$$

Here we have used (Fig. 1)

$u = l\cos\theta, \quad v = l\sin\theta$

$s = x\cos\theta + y\sin\theta\,.$

Taking Fourier transforms of both sides of Eq. (8) yields

$$\int_{-\infty}^{+\infty} \varepsilon(s,\theta)\, e^{-\mathrm{i}\,2\pi ls}\, ds = \iint_{-\infty}^{+\infty} \partial\varrho^*(x,y)/\partial s\, e^{-\mathrm{i}\,2\pi ls}\, ds\, dt\,,$$

or

$$E(l,\theta) = \mathrm{i}\,2\pi l\, R(l,\theta)\,.$$

Therefore,

$$R(l,\theta) = E(l,\theta)/(\mathrm{i}\,2\pi l)\,. \tag{A3}$$

The inverse Fourier transform of (A2) in polar coordinates gives

$$\varrho^*(x,y) = \int_0^{\pi}\int_{-\infty}^{+\infty} R(l,\theta)\, e^{\mathrm{i}\,2\pi ls}\,|l|\, dl\, d\theta\,. \tag{A4}$$

Here we have changed the integral limits $(0, 2\pi)$ to $(0, \pi)$ in θ, $(0, \infty)$ to $(-\infty, \infty)$ in l, and l (always positive) to $|l|$ in the Fourier transform domain.

Substituting (A3) into (A4), we have

$$\varrho^*(x,y) = \int_0^{\pi} d\theta \int_{-\infty}^{+\infty} Q(l)\, E(l,\theta)\, e^{\mathrm{i}\,2\pi ls}\, dl\,, \tag{A5}$$

where $Q(l) = |l|/(\mathrm{i}\,2\pi l)\,.$

Using the definition of convolution, (A5) becomes

$$\varrho^*(x,y) = \int_0^{\pi} q(s) * \varepsilon(s,\theta)\, d\theta\,, \tag{9}$$

where

$$q(s) = \int_{-\infty}^{+\infty} Q(l)\, e^{\mathrm{i}\,2\pi ls}\, dl$$

is the filtering function.

Equation (9) is the solution of Eq. (8), and serves as the basic equation for computer programming.

The sampling interval in the space domain is taken to be Δs, which corresponds to a cut-off frequency in the Fourier transform domain

$l_c = 1/(2\Delta s)\,.$

Therefore,

$$q(s) = \int_{-\infty}^{+\infty} Q(l)\, W(l)\, e^{\mathrm{i}\,2\pi ls}\, dl\,,$$

where $W(l)$ is a window function in the Fourier transform domain

$$W(l) = \begin{cases} 1, & \text{when } |l| \le l_c \\ 0, & \text{otherwise} \end{cases}.$$

Then,

$$\begin{aligned} q(s) &= \int_{-l_c}^{+l_c} |l|/(\mathrm{i}\,2\pi l)\, e^{\mathrm{i}\,2\pi ls}\, dl \\ &= \pi^{-1}\int_0^{l_c} \sin(2\pi ls)\, dl \\ &= [1 - \cos(\pi s/\Delta s)]/(2\pi s)\,. \end{aligned}$$

Since $s = m\Delta s$, we obtain the filter function in a form as

$$\begin{aligned} q(s) &= (\pi\Delta s)\,[(1 - \cos m\pi)/2m] \\ &= (\pi^2\Delta s)^{-1}\, q(m)\,, \end{aligned}$$

where the discretized filter function is

$$q(m) = \begin{cases} 1/m, & \text{when } m = \text{odd} \\ 0, & \text{otherwise} \end{cases} \quad (11)$$

Using the trapezoidal rule for the numerical integration of equation (A6), we have

$$\varrho^*(k\Delta x, n\Delta y) = \Delta\theta\Delta s \sum_{j=0}^{N-1} \sum_{m'=-(M-1)/2}^{(M-1)/2} \varepsilon(m'\Delta s, j\Delta\theta)\, q((m-m')\Delta s). \quad (A6)$$

Since $\Delta\theta = \pi/N$, the substitution of (11) into (A6) yields

$$\varrho^*(k\Delta x, n\Delta y) = (N\pi)^{-1} \sum_{j=0}^{N-1} \sum_{m'=-(M-1)/2}^{(M-1)/2} \varepsilon(m'\Delta s, j\Delta\theta)\, q(m-m'). \quad (10)$$

This is the basic discretized equation for the tomographic reconstruction of the relative helium density distribution.

References

Blinkov, G. N.; Fomin, N. A.; Soloukhin, R. I. 1987: Multidirection speckle photography of density gradients in a flame. Paper presented at 11th Int. Coll. on Gasdynamics of Explosions and Reactive Systems, Warszawa, Poland

Debrus, S.; Françon, M.; Grover, C. P.; May, M.; Roblin, M. L. 1972: Ground glass differential interferometer. Appl. Opt. 11, 853–857

Erbeck, R.; Keller, J. 1987: Image processing of Young's fringes in laser speckle velocimetry. In: The use of computers in laser velocimetry (eds. Pfeifer, H. J.; Jaeggy, B.) pp. 26/1–26/5. St. Louis, France: ISL

Faris, G. W.; Byer, R. L. 1987: Beam-deflection optical tomography. Opt. Lett. 12, 72–74

Herman, G. T. 1980: Image reconstruction from projections. New York: Academic Press

Hesselink, L. 1989: Optical tomography. In: Handbook of flow visualization (ed. Yang, W.-J.). Washington/DC: Hemisphere

Köpf, U. 1972: Application of speckling for measuring the deflection of laser light by phase objects. Opt. Commun. 5, 347–350

Merzkirch, W. 1987: Flow visualization, 2nd edn. New York: Academic Press

Snyder, R.; Hesselink, L. 1984: Optical tomography for flow visualization of the density field around a revolving helicopter rotor blade. Appl. Opt. 23, 3650–3656

Sweeney, D. W.; Vest, C. W. 1973: Reconstruction of three-dimensional refractive index fields from multi-directional interferometric data. Appl. Opt. 22, 2649–2664

Wernekinck, U.; Merzkirch, W. 1987: Speckle photography of spatially extended refractive-index fields. Appl. Opt. 26, 31–32

Received August 30, 1988